3D MHD simulations of unmitigated Vertical Displacements Events in ITER

F.J. Artola[1], A. Loarte[1], M. Hoelzl[2], N. Schwarz[2], M. Lehnen[1], R.A. Pitts[1] and the JOREK team[3]

[1] *ITER Organization, St. Paul Lez Durance, France*

[2] *Max Planck Institute for Plasmaphysics, Garching, Munich*

[3] *please refer to [M Hoelzl, G T A Huijsmans, S J P Pamela, M Becoulet, E Nardon, F J Artola, B Nkonga et al, Nuclear Fusion 61, 065001 (2021)]*

One of the high priority research needs for the ITER project is the development of a solid physics basis for plasma disruptions and their mitigation. Present predictions for the thermal and electromagnetic loads caused by unmitigated Vertical Displacement Events (VDEs) rely on experimental observations and axisymmetric simulations [1]. 3D effects, such as the sideways vacuum vessel (VV) force produced by toroidally asymmetric VDEs, must be understood to provide the basis for load validation in support of the ITER Research Plan and to make predictions for full current operation. Previous 3D simulations of ITER unmitigated VDEs reported a maximum sideways force of $F_h \sim 30$ MN [2], but the plasma current evolution $I_p(t)$, as well as the Thermal Quench (TQ) were artificially imposed. In this paper, we provide simulations of the TQ phase as well as the initial Current Quench (CQ) phase for an ITER 15 MA unmitigated VDE. The novelty of this work is that the TQ occurs naturally and the evolution of I_p and the edge safety factor (q_{95}) is calculated self-consistently. Special attention is paid to the TQ onset, TQ duration and the heat-flux decay length λ_q during the TQ. The initial phase of the CQ is also analysed, with particular interest in the evolution of q_{95}. It is thought that the cause of the sideways force is the growth of a 1/1 MHD mode which occurs once q_{95} drops to a value of 1, and thus, a key question is how q_{95} reaches unity considering that the disruptive kink limit occurs already at $q_{95} \sim 2$.

To address these issues, the MHD code JOREK [3, 4] is employed together with the STARWALL code [6] that includes the effect of coils and passive conductors. The included ITER relevant passive conductors are taken as in [7]. The initial condition for the presented simulations is an ITER 15 MA L-mode reference equilibrium modelled with CORSICA [5]. The following Dirichlet boundary conditions were chosen at the plasma-

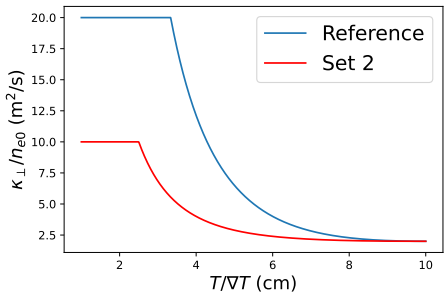

Figure 1: *Perpendicular thermal conductivity coefficients with* $n_{e0} = 5.4 \times 10^{19}\ m^{-3}$.

wall interface $T_e = 1$ eV, $n_e = 1.1 \times 10^{19}$ m^{-3} and no normal-flow conditions [7]. Although JOREK has different model extensions, here we use the single temperature model without impurities employed in [7] but including the Ohmic heating term. Validation activities for this model with unmitigated ASDEX-Upgrade VDE experiments can be found in [8].

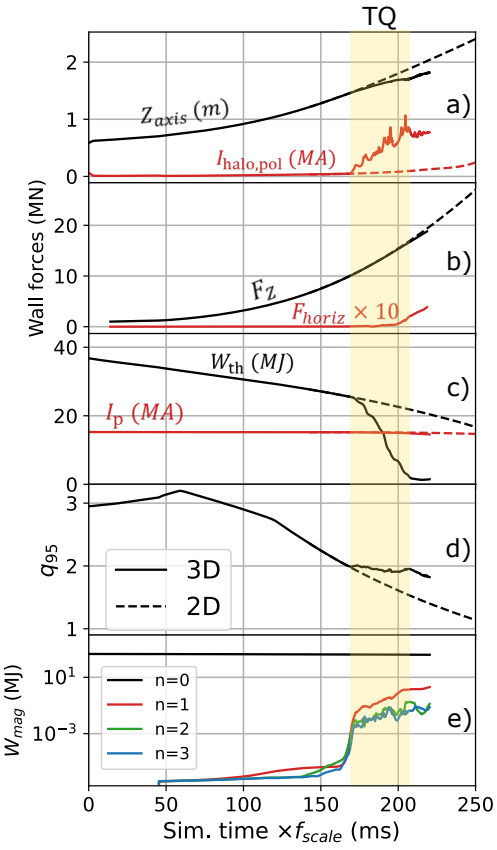

Figure 2: *Reference upward VDE evolution with $f_{scale} = 20$ and $\kappa_\parallel^{min} = \kappa_\parallel(30eV)$. (a) Vertical position and poloidal halo current. (b) Integral VV forces. (c) Thermal energy and total plasma current. (d) Edge safety factor. (e) Poloidal magnetic energy for different toroidal mode numbers. The dashed lines represent an axisymmetric run without a TQ.*

Since unmitigated VDEs in ITER are expected to occur on time-scales given by the wall time ~ 500 ms, complete 3D JOREK simulations with present capabilities imply years of runtime. To make the simulations computationally feasible, we choose a set of expected parameters for an ITER L-mode plasma (see Table 1 and Figure 1) and rescale them by a common factor f_{scale}. The rescaled parameters are (η, η_w, D, $\kappa_\perp$, $\kappa_\parallel$) so that the characteristic diffusion times of current, particles and energy become f_{scale} times shorter. This reduces the computational cost since the simulation time step is typically determined by the Alfvén time. The rescaling procedure gives an identical evolution (but with the time axis scaled) to axisymmetric (2D) simulations with realistic parameters.

For the VDE initiation and direction, a current perturbation of ± 20 kA is applied in the in-vessel vertical stability coils (VS3). Next, the plasma moves vertically on a time-scale given by the wall time at roughly constant I_p (see Figure 2 a, c) since the plasma temperature remains sufficiently high. The shrinkage of the plasma volume caused by the VDE and the constancy of I_p causes a drop in q_{95} (since $q_{95} \propto a^2/I_p$). Once q_{95} approaches a value of 2, low$-n$ external kink modes become unstable at the plasma edge, which lead to the TQ onset (see Figure 2 c, d, e). In addition, a 1/1 core mode develops due to the presence of a $q = 1$ surface inside the plasma. The growth of the external kink modes causes a stochastic field line front that propagates from the plasma edge to the core. The temperature decreases in the open field line region until parallel conduction becomes no longer effective.

The latter can be observed in Figure 3, where the transition to closed field lines is correlated with a change in the T_e gradient. The stochastic front does not penetrate all the way to the magnetic axis and stops approximately at half-radius. The final core temperature collapse is caused by the 1/1 mode which enhances the core transport.

Parameter	Value	Description
D	2 m^2/s	Isotropic particle diffusion
$\kappa_\perp$	∇T-dependent (see Figure 1)	Perp. thermal conductivity
$\kappa_\parallel$	Spitzer-Haerm $\propto T_e^{5/2}$ $\kappa_\parallel^{max} = \kappa_\parallel(0.3/1\,\mathrm{keV})$ $\kappa_\parallel^{min} = \kappa_\parallel(1/30\,\mathrm{eV})$	Parallel thermal conductivity
η	Spitzer $\propto T_e^{-3/2}$ with $Z_{eff} = 1.12$ $\eta^{max} = \eta(1\mathrm{eV})$ $\eta^{min} = \eta(300/\infty\mathrm{eV})$	Parallel resistivity
η_w/d_w	$13.3\,\mu\Omega$	Wall resistivity over thickness
$(\nu_\perp, \nu_\parallel)$	(2, 297) m^2/s	Perp./Parallel viscosity

Table 1: *Unscaled simulation parameters. Red values correspond to the cases labelled as "Set 2". The values for ν are evaluated for a density of* $n_{e0} = 5.4 \times 10^{19}\ m^{-3}$.

The dependence of the TQ duration on f_{scale} is studied in order to extrapolate to ITER parameters. We define the TQ duration $\tau_{TQ}^{W_{th}}$ by using the times where the thermal energy decays from 90% to 20% of the pre-TQ value as it was defined in [9].

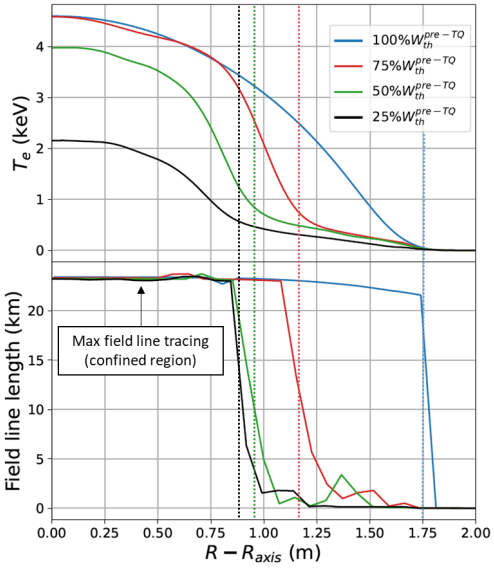

Figure 3: *(Upper) Electron temperature profile at the Z_{axis} midplane. (Lower) Traced field line length before intersecting the first wall for different points in the midplane. The line colors correspond to time instances with different fractions of the pre-TQ thermal energy. The dashed lines indicate the transition between open and closed field lines.*

The results shown in Figure 4 a) suggest that $\tau_{TQ} \propto f_{scale}^{-1}$ and that predicted values for ITER parameters will be larger than 10 ms (up to 60 ms). However impurity radiation is not included in this work, and therefore these values represent upper limits. The maximum $n = 1$ growth rate in the linear phase is found to scale with f_{scale}, which is consistent with $\tau_{TQ} \propto f_{scale}^{-1}$ if the stochastic front propagation is given by the $n = 1$ growth. Such growth rate scaling is similar to the RWTM scaling proposed by [10], which gives $\gamma \propto f_{scale}^{0.8}$.

When using the drop of the core temperature to characterize the TQ duration, a big scatter in $\tau_{TQ}^{W_{th}}/\tau_{TQ}^{T_{e,core}}$ is found in the simulations (0.8-6.5) as well as in JET VDE experiments (1-4) [9].

To characterize the heat flux decay length during the TQ (λ_q), we use the following definition to define a toroidally averaged decay length $<\lambda_q>$

$$<\lambda_q> = \frac{P_{\mathrm{SOL}}}{4\pi R_{\mathrm{LCFS}}^{\mathrm{OMP}} (B_\theta/B_\phi)^{\mathrm{OMP}} \max(<q_\parallel^{\mathrm{OMP}}>)} \quad (1)$$

where "OMP" denotes that quantities are evaluated at the outer midplane, P_{SOL} is the total

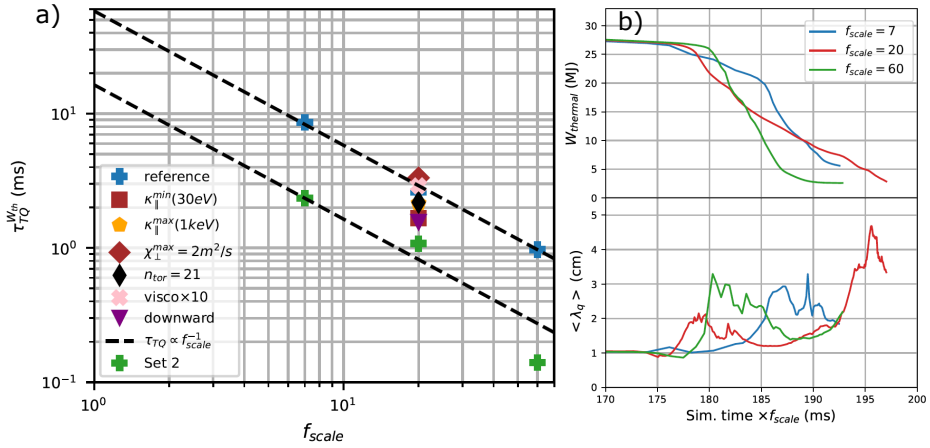

Figure 4: *(a) TQ duration as a function of f_{scale} for different parameter variations. (b) Time traces of the thermal energy and $< \lambda_q >$ for different f_{scale} values for the "Set 2" parameters.*

thermal power reaching the first wall, $R_{\mathrm{LCFS}}^{\mathrm{OMP}}$ is the major radius at the plasma boundary and $< q_{\parallel}^{\mathrm{OMP}} >$ is the toroidal average of the parallel heat flux mapped from the first wall to the OMP. The chosen diffusion parameters lead to a pre-TQ $< \lambda_q > \sim 1$ cm for the set of parameters "Set 2" (which has less restricting thresholds) as indicated in Figure 4 b). During the TQ, $< \lambda_q >$ expands to 2-3 cm without a clear dependence on f_{scale}.

Finally we note that the MHD activity during the TQ is able to pause the decay of q_{95} by inducing halo currents (Figure 2 a,d). After the TQ, q_{95} continues to decay at a similar rate as in the axisymmetric simulation despite the continued growth of the $n = 1$ mode. This points to the possibility of attaining $q_{95} = 1$ in ITER leading to large horizontal VV forces. The simulations must continue to assess this issue, but the strong non-linearities pose a challenging convergence to the JOREK solver.

Acknowledgements ITER is the Nuclear Facility INB No. 174. This work explores the physics processes during plasma operation of the tokamak when disruptions take place; nevertheless the nuclear operator is not constrained by the results presented here. The views and opinions expressed herein do not necessarily reflect those of the ITER Organization. The simulations presented here have been performed using the JFRS-1 and the ITER HPC clusters. This work has been carried out within the framework of the EUROfusion Consortium, funded by the European Union via the Euratom Research and Training Programme (Grant Agreement No 101052200 — EUROfusion). Views and opinions expressed are however those of the author(s) only and do not necessarily reflect those of the European Union or the European Commission. Neither the European Union nor the European Commission can be held responsible for them.

References

[1] M. Lehnen, et al., Journal of Nuclear Materials **463**, 39-48 (2015)

[2] H. Strauss, Physics of Plasmas **25**, 2 (2018)

[3] G. T. A. Huysmans, and O. Czarny, Nuclear fusion **47**, 7 (2007)

[4] M. Hoelzl, et al., Nuclear Fusion **61**, 6 (2021)

[5] S.H. Kim, et al, Nuclear Fusion **57**, 8 (2017)

[6] P. Merkel, and E. Strumberger, arXiv preprint arXiv:1508.04911 (2015).

[7] F.J. Artola, et al, Nuclear Fusion **62**, 5 (2022)

[8] N. Schwarz, et al, 48th EPS Conference on Plasma Physics I3.101 (2022)

[9] G. Arnoux, et al, Nuclear Fusion **49**, 8 (2009)

[10] H. Strauss, Physics of Plasmas **28**, 7 (2021)